Icarus 311 (2018) 258–270

Contents lists available at ScienceDirect

Icarus

journal homepage: www.elsevier.com/locate/icarus

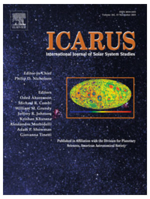

The lunar surface around extremely fresh craters

Vadym Kaydash[a], Yuriy Shkuratov[a,*], Viktor Korokhin[a], Sergey Velichko[a], Gorden Videen[b]

[a] Institute of Astronomy, Kharkov V.N. Karazin National University, Kharkov 61022, Ukraine
[b] Space Science Institute, 4750 Walnut St. Suite 205, Boulder, CO 80301, USA

ARTICLE INFO

Article history:
Received 23 October 2017
Revised 15 April 2018
Accepted 17 April 2018
Available online 18 April 2018

Keywords:
Moon
Surface
Photometry
Regolith

ABSTRACT

We investigate surface changes near two lunar craters formed on March 17 and September 11, 2003, using high-resolution imagery data (0.5 m/pixel) of the LRO narrow angle camera. The phase- and temporal ratio techniques are applied. Using these techniques reveals a slight “butterfly-wings” pattern around the March 17 crater. This pattern is not seen on usual brightness images. The observed dark halos around the craters may be formed by thin deposits of vapor products at the impacts. Rough estimates show that only 100 g of the nano-phase iron (npFe^0) is needed to generate the darkening effect, if the iron is spread in a layer of 10 nm thickness on an area with a radius of 70 m. A portion of the ejected materials is seen around the craters as dark and bright splotches. The dark splotches could be produced when excavated material interacts with the cloud of evaporated substance and then falls down to the surface.

1. Introduction

In the past, meteoroid impacts played a significant role in the formation of the Solar System. These phenomena are still active today on relatively small scales, producing unexpected Chelyabinsk-like events on the Earth or new small craters on the Moon. Such craters with sizes on the order of 10–100 m usually are bowl-shaped and have no terraced crater rims, or flat floors and central peaks (e.g., Melosh, 1996). They may reveal bright halos and rays that are widely known as a result of excavation of subsurface materials. Since fresh materials ejected from craters consist of immature soils, they are generally brighter than the surrounding region. A smaller number of dark-haloed and dark-rayed small craters on the Moon also have been observed. It is considered that these may relate to the excavation of dark subsurface materials (e.g., Schultz and Spudis, 1979) and/or high roughness of the ejecta blanket surface (Kaydash et al., 2014). At oblique impacts “butterfly-wings” ejecta patterns can be observed around some craters (Gault and Wedekend, 1978; Melosh, 1996) that also are rather rare.

Recent impact events on the lunar nearside are detected with several lunar monitoring programs searching for the flashes caused by meteoroid impacts. Among those programs are both amateur and professional surveys (e.g., Perna et al., 2013; Madiedo et al., 2014; Suggs et al., 2014). To study such flashes, ground telescopes of small apertures equipped with sensitive cameras usually are used. NASA’s Lunar Impact Monitoring Program allowed the detection of impact flashes using the facility at Marshall Space Flight Center (Suggs et al., 2014). The MSFC program of video monitoring the earthshine portion of the Moon has detected over 300 lunar impacts since 2006 (Suggs et al., 2014). The project named MIDAS (Moon Impacts Detection and Analysis System) has been running since 2009 with the same aim to record impact flashes (Madiedo et al., 2014).

The brightest flash recorded by MSFC facility occurred on 17 March 2013 (e.g., Robinson et al., 2015). Later in that year, MIDAS also recorded an extraordinary flash in the western part of Mare Nubium on September 11. Suggs et al., (2014) estimated the 17 March 2013 impactor to have a speed of 25.6 km/s and a mass of 16 kg and estimated the crater diameter to be 12–20 m. The MIDAS team (Madiedo et al., 2014) has analyzed the September 11, 2013 impact event assessing the crater diameter to be 47–56 m. When these craters were found on the Moon, their diameters were found to be 19 and 34 m, respectively.

Hundreds of new craters of several tens of meters in size can be identified using the Narrow-angle camera (NAC) images acquired during NASA’s Lunar Reconnaissance Orbiter (LRO) mission, which has a spatial resolution of 0.5 m from its 50-km orbits (Robinson et al., 2010). Studying very fresh lunar craters is important, since their degradation degree is minimal, and, hence, the original roughness of the ejecta blanket and very thin deposits, e.g., resulting from the impact metamorphism of the crater substances, can be investigated. LROC NAC images of such craters allow an examination of the subsurface structure of the Moon, since the distance of the ejected material correlates with its depth before the impact (e.g., Melosh, 1996).

---

* Corresponding author.
E-mail address: yuriy.shkuratov@gmail.com (Y. Shkuratov).

https://doi.org/10.1016/j.icarus.2018.04.024

We here consider two new lunar craters using LROC NAC images acquired before and after the impacts on March 17 and September 11, 2013. In our studies, we use the phase-ratio technique proposed by Shkuratov et al., (1994, 2011, Shkuratov et al. 2012a) and Kaydash et al., (2011, Kaydash et al. 2012). The gist of the method relates to the brightness dependence on the phase angle α. Particulate surfaces, including lunar regolith, show prominent backscattering of light. The backscattering is described by the phase function $f(\alpha)$. The slope of the phase function depends on the complexity of the surface structure and surface albedo (Shkuratov et al., 2011; Hapke, 2012; Kaydash et al., 2012). The simplest approach for analyzing phase functions over a surface is to image the phase ratio $f(\alpha_1)/f(\alpha_2)$, i.e. the ratio of coregistered images acquired at different phase angles. The image coregistration implies that corresponding pixels representing the same objects can be compared. Sometimes such a corregistering is not a trivial problem, since the images are acquired at diverse projections and scales; and the same details may differ from each other. Various algorithms can be used in this situation, in particular, the "rubber-sheet" technique based on an assessment of the local correlation in a small sliding window (Kaydash et al., 2012).

Phase-ratio imagery allows one to suppress the inherent albedo variations of the surface, which results in $f(\alpha)$ slope dependence on the surface roughness. For different combination of α_1 and α_2 the roughness influence is different. At small scales the packing density of a particulate surface is an important characteristic, however, at much larger scales the ratio $f(\alpha_1)/f(\alpha_2)$ also can be a function of surface topography (Kaydash et al., 2012). All changes in surface roughness that can be detected with optical methods we call optical roughness.

The ratios of photometric images obtained before and after an impact event at the same illumination/observation conditions (temporal ratios) also suggests a unique technique to study changes of the surface properties. We here used the ratios (A/B) that means After/Before the impact event. The ratio image is homogeneously grey, if the impact does not disturb the brightness pattern. Dark and bright details of the ratio image correspond to a disturbance of the surface composition and roughness. The temporal ratio technique helps to separate the initial albedo distribution and the brightness pattern caused by impact effects.

Mapping slopes of the phase functions can be a very effective tool to study the lunar surface structure, since such imagery allows one to estimate variations of the complexity of unresolved surface roughness and microtopography. This method has been applied to studies of the crater Giordano Bruno (Shkuratov et al., 2012a), young craters near the crater Denning and in the Balmer basin, in addition to the craters created by the impacts of the Ranger-6 spacecraft and Saturn-5 sections of Apollo-13 and Apollo-17 missions (Kaydash and Shkuratov, 2012; Kaydash et al., 2014). This technique also has been used for investigations of the Soviet Luna-16, Luna-20, and Luna-24 landing sites (Kaydash et al., 2013; Shkuratov et al., 2013a) as well as large photometric anomalies (Korokhin et al., 2016) found with Earth-based telescope observations (Shkuratov et al., 2010). Robinson et al., (2015) also used the phase-angle technique, showing, in particular, that although the new crater formed on March 17, 2013 is about 1919 meters m in size, its influence is large: traces of excavated material can be seen at hundreds of meters and some surficial changes have been detected even up to 30 km away.

2. Data and processing

We consider here temporal and phase-ratio images. The first type allows one to compare two images and, hence, to detect changes that occurred in the frame due to, e.g., an impact event. The second one allows us to compare the same scene at different photometric conditions. The construction of temporal and phase ratios demands preliminary processing and a unification of source images. For instance, for the temporal ratios it is very desirable to use the components with the same illumination/observation conditions. As for phase ratios, the components are inevitably different photometrically because of the phase angle α. However, the most reliable results can be obtained if the difference in α is due only to the viewing angle at equal azimuth and incident angles; in this case parallax distortions are observed, but these distortions can be compensated by applying the mentioned rubber-sheet algorithm (Kaydash et al., 2012), when the final coregistration of images with subpixel accuracy is performed by local shifts that are found by maximizing the local correlation between frames. The parallax data, obtained from the applying the rubber-sheet algorithm, allow one to construct anaglyphs of scenes (Kaydash et al., 2012) and even photoclinometry studies.

Slopes of the phase function $f(\alpha)$ at various phase angles are controlled mainly by the shadowing effect that increases with increasing surface roughness (e.g., Shkuratov et al., 2011; Hapke, 2012). The reflectance (albedo) of a rough surface depends on multiple light scattering: the higher the component of multiple scattering, the higher the albedo is. The Moon is dark, and therefore, the multiple scattering component, which produces illumination in shadows, is rather secondary for the Moon; although, in general, the albedo factor may noticeably influence the $f(\alpha)$ slope. Ejecta areas of the youngest craters may have surfaces that are rougher than their surroundings, as the crater halos and rays are zones of surface disturbance. Thus, the phase-ratio technique is very suitable as a tool for assessment of optical roughness.

In the lunar site where the brightest flash occurred on 17 March 2013, a new 18.8-m diameter crater (20.7135°N, 335.6698°E) was found by Robinson et al., (2015). After the 11 September 2013 bright flash the LROC team found a new crater ~34 m in diameter with coordinates 17.167°S, 339.599°E (M. Robinson, http://lroc.sese.asu.edu/posts/810). There are several suitable images acquired by the LROC NAC before the impact, making possible a photometric investigation of the new crater and its ray system. Table 1 lists all the images we use for temporal and phase-ratio imagery in this work.

We process the selected NAC images by converting raw data into radiance factor, making selenographic reference and calculation of photometric angles for each pixel in the frames. For this we use the ISIS software (isis.astrogeology.usgs.gov) with the latest SPICE kernels (naif.jpl.nasa.gov/pub/naif/pds/data/lro-ll-spice-6-v1.0/lrosp_1000). To derive phase-function slopes we perform coregistering of two suitable images with sub-pixel accuracy and obtain the phase-ratio image by dividing their corresponding pixels (e.g., Kaydash et al., 2012). Each of the frames constituting phase and temporal ratios is reduced to the standard photometric conditions through division by the Lommel–Seeliger factor $\cos i \ / \ (\cos e + \cos i)$, where i and e are incident and emission angles, respectively. Although this factor is not the best for photometric corrections (e.g., Shkuratov et al., 2011, Shkuratov et al. 2012b, 2013b), it is very simple and works well, when variations of i and e inside of frames are rather small. All the frames are mapped into a common cartographic projection with an effective spatial resolution of 1 m/pix.

The NAC images are subjected to the echo-effect that was discovered in the summer of 2011 in the NAC detectors. This effect relates to the high speed (>3000 lines/second) of the NAC detectors. The signal in each pixel is replicated to a smaller extent in the pixel on the same line (http://isis.astrogeology.usgs.gov/Application/presentation/Tabbed/lronacecho/lronacecho.html). The ISIS software offers the *lronacecho* application, which removes this effect from the data. We also apply this correction with the default parameter values.